J. Fluid Mech. (1995), *vol.* 291, *pp.* 263–285

A slender ship moving at a near-critical speed in a shallow channel

By XUE-NONG CHEN† AND SOM DEO SHARMA
Department of Marine Technology, Mercator University, Duisburg, Germany

(Received 22 January 1993 and in revised form 26 October 1994)

The problem solved concerns a slender ship moving at a near-critical steady speed in a shallow channel, not necessarily in symmetric configuration, involving the special phenomenon of generation of solitary waves. By using the technique of matched asymptotic expansions along with nonlinear shallow-water wave theory, the problem is reduced to a Kadomtsev–Petviashvili equation in the far field, matched with a near-field solution obtained by an improved slender-body theory, taking the local wave elevation and longitudinal disturbance velocity into account. The ship can be either fixed or free to squat. Besides wave pattern and wave resistance, the hydrodynamic lift force and trim moment are calculated by pressure integration in the fixed-hull case; running sinkage and trim, by condition of hydrodynamic equilibrium in the free-hull case. The numerical procedure for solving the KP equation consists of a finite-difference method, namely, fractional step algorithm with Crank–Nicolson-like schemes in each half step. Calculated results are compared with several published ship-model experiments and other theoretical predictions; satisfactory agreement is demonstrated.

1. Introduction

It was observed in several early studies (e.g. Thews & Landweber 1935, 1936; Kinoshita 1946; Graff 1962; Graff, Kracht & Weinblum 1964) that, surprisingly, the flow around a steadily towed ship model does not attain a steady state even in a long tank if the constant towing speed U^* lies near the natural speed of a long wave, i.e. so-called critical speed, $(g^*h^*)^{1/2}$, where g^* is the acceleration due to gravity and h^* is the still water depth. Recent towing tank experiments (Huang, Sibul & Wehausen 1983; Ertekin, Webster & Wehausen 1985) show that instead of reaching the expected steady state the ship model generates periodic solitary waves in front of itself, which travel a bit faster than the model. Consequently, the hydrodynamic forces acting on the model, namely, resistance, lift and trim moment also vary periodically, resulting in a periodic heave and pitch motion if these two modes are free.

The recent theoretical interest and a new understanding of the problem stem from the work of Wu & Wu (1982), who used one-dimensional Boussinesq equations to study a pressure patch moving on the free surface at a near-critical speed and found upstream solitons emitted periodically. Since then various investigations have followed. Calculations for a surface pressure or bottom disturbance were performed by Ertekin (1984) and Ertekin *et al.* (1985, 1986) using Green–Naghdi's directed-sheet model; by Akylas (1984) and Cole (1985) using Korteweg–de Vries equation with a forcing term; by Katsis & Akylas (1987) using Kadomtsev–Petviashvili equation; and so on. All

† Present address: University of Stuttgart, Math. Inst. A, D-70569 Stuttgart, Germany.

yield qualitatively similar results. Subsequently, this problem was analysed by Grimshaw & Smyth (1986) and Smyth (1986) applying the modulation theory of Whitham (1974). A preliminary study was also made by Wu (1987) who approximately analysed the forced KdV equation to ascertain the mechanism underlying the phenomenon.

For a real ship problem, unlike other kinds of disturbance, its three-dimensional geometry must be taken into account. Mei (1986) derived an inhomogeneous KdV equation with matched asymptotic expansions to analyse a slender ship hull and obtained solitary waves propagating upstream. Mei & Choi (1987) further developed the above theory to calculate hydrodynamic forces on the ship, but only crude agreement with experiment was obtained because this theory cannot predict two-dimensional waves in the wake. Choi & Mei (1989) improved their theoretical model by using a KP equation in the far field to take account of the two-dimensional effect. More numerical results were reported in Choi *et al.* (1990) based on the classical Hamilton's principle together with another finite-element method for numerical calculation. It seems to us that this approach is worth pursuing further, but it should be improved by taking the actual submerged cross-sectional area of the ship and other higher-order effects in the near field into account. Moreover, it can be extended to the asymmetric case, allowing determination of side force and yaw moment on a ship moving in a canal on an off-centre track or at a slight angle of yaw.

From an applications point of view, with recently increasing interest in fast inland and coastal ships, the demand for clarifying shallow and restricted water effects on ships is stronger than ever before. As described in many papers (e.g. Graff *et al.* 1964; Dand 1973), the wave resistance of a ship increases steeply with speed as it approaches the critical Froude number, reaching a maximum value at a near-critical speed still in the subcritical range. Meanwhile, the squat phenomenon takes place so that the ship may touch ground. Beyond that point the wave resistance first decreases and then increases again slowly. Tuck (1966) developed a technique of matched asymptotic expansions based on linearized shallow-water wave theory to construct an approximate solution. This approximation gives fair results for ship squat at depth Froude numbers not close to unity but is singular and therefore invalid near $F_{nh} = 1$. The linearized theory fails to predict wave resistance in this transcritical range not only because the wave amplitude is no longer small but also because it cannot predict the nonlinear phenomenon of periodic bifurcation from a steady state. Some attempts based on nonlinear theory were undertaken by Lea & Feldman (1972) and Mei (1976) for the same case but still pursuing a steady state solution.

Here it seems appropriate to insert a comment on slender-body theory in shallow water. Almost all previous investigators (Tuck 1966; Lea & Feldman 1972; Mei 1976, 1986; Choi & Mei 1989) who used matched asymptotic expansions in conjunction with linear or nonlinear shallow-water wave theory, applied the lowest-order slender-body theory in the near field, i.e. approximated the free surface around the ship by a rigid wall at $z = 0$ and the longitudinal flow past the body by the uniform parallel inflow. Then the flux to the outer flow is simply proportional to the local slope of the still-water cross-sectional area. However, some investigators (Ogilvie 1976; Maruo 1989) recognized that this original slender-body theory in deep water neglects two not-so-small effects: (i) interaction between waves generated at different cross-sections; (ii) longitudinal perturbation velocity in the linearized body boundary condition. Maruo (1989) improved the slender-body theory by a rational perturbation analysis and apparently including the above two effects obtained somewhat better results for wave resistance and wave elevation than the older theory. Following these suggestions, we

also account for these two effects in our slender-body approximation in the near field and believe this to be consistent with the nonlinear shallow-water wave theory in the far field. In contrast to the far-field problem, there is no resonant point in the near-field problem, i.e. no mathematical singularity. We can just apply the regular perturbation method there. So if we want to obtain the same accuracy in the near-field as in the far-field nonlinear theory, the near-field solution must contain terms of different orders. Consequently, there are higher-order terms in the matching condition.

This paper is aimed at developing a practical and efficient calculation method by further exploiting the idea proposed by Choi & Mei (1989). Considering a ship moving at a near-critical speed parallel to the sidewalls but not necessarily in the centreplane of a shallow rectangular channel, using the technique of matched asymptotic expansions along with nonlinear shallow-water wave theory, we reduce the problem to a KP equation in the far field, matched with a near-field solution obtained by improved slender-body theory of higher-order precision, taking account of local wave elevation and longitudinal disturbance velocity. The KP equation is solved numerically by a finite-difference method, namely, the fractional step algorithm with Crank–Nicolson-like schemes in each half step. The generated waves and associated hydrodynamic forces on the ship, namely, wave resistance, lift force and trim moment, are calculated. If the ship model is free to heave and pitch, the running sinkage and trim of the ship are obtained at each timestep from the condition of quasi-steady hydrodynamic equilibrium, i.e. zero net lift-force and trim-moment ignoring inertial effects. Exemplary results for three hull forms, namely, Series 60 $C_B = 0.8$, Taylor Standard Series and Wigley model, are presented along with corresponding results from published experiments (Graff *et al.* 1964; Ertekin *et al.* 1985; Millward & Bevan 1986) and theoretical predictions (Choi *et al.* 1990; Millward & Bevan 1986). Satisfactory agreement between the experiments and our calculations is demonstrated. It is inferred that the method based on nonlinear shallow-water wave theory holds enough precision for the practical ship problem if certain higher-order effects in the near field are taken into account.

2. Formulation

2.1. *General description of the problem*

We consider asymptotically a slender ship of length l^*, beam b_0^* and draft d^* moving along the x^*-direction in a shallow channel of depth h^* and width w^* at a near-critical speed U^*. The flow is assumed to be irrotational and incompressible; the ship, free only to heave and pitch. We start with dimensional variables marked by asterisks and will later change to unmarked non-dimensional variables. A Cartesian coordinate system $Ox^*y^*z^*$ moving at the same speed as the ship is used with origin O located in the midship section, plane Ox^*y^* on the quiet free surface, plane Ox^*z^* as longitudinal ship centreplane, z^* positive upward, and x^* positive forward. The flow is then exactly governed by the Laplace equation in the fluid domain,

$$\frac{\partial^2\phi^*}{\partial u^{*2}}+\frac{\partial^2\phi^*}{\partial y^{*2}}+\frac{\partial^2\phi^*}{\partial z^{*2}}=0 \quad (-h^*<z^*<\zeta^*), \tag{1}$$

by the kinematic and dynamic conditions on the free surface,

$$\frac{\partial\zeta^*}{\partial t^*}-U^*\frac{\partial\zeta^*}{\partial x^*}+\frac{\partial\phi^*}{\partial x^*}\frac{\partial\zeta^*}{\partial x^*}+\frac{\partial\phi^*}{\partial y^*}\frac{\partial\zeta^*}{\partial y^*}=\frac{\partial\phi^*}{\partial z^*} \quad (z^*=\zeta^*), \tag{2}$$

$$\frac{\partial \phi^*}{\partial t^*} - U^* \frac{\partial \phi^*}{\partial x^*} + \tfrac{1}{2}|\nabla^* \phi^*|^2 + g^* z^* = 0 \quad (z^* = \zeta^*), \tag{3}$$

and by the boundary conditions on the channel bottom,

$$\frac{\partial \phi^*}{\partial z^*} = 0 \quad (z^* = -h^*), \tag{4}$$

on the channel sidewalls,

$$\frac{\partial \phi^*}{\partial y^*} = 0 \quad (y^* = -\lambda w^* \text{ and } (1-\lambda) w^*), \tag{5}$$

and on the ship hull,

$$\frac{\partial F}{\partial t^*} - U^* \frac{\partial F}{\partial x^*} + \nabla^* \phi^* \cdot \nabla^* F = 0 \quad (F(x^*, y^*, z^*, t^*) = 0), \tag{6}$$

where ϕ^* is the disturbance velocity potential of fluid, ζ^* is the elevation of free surface, and λ is a symmetry parameter having positive real values less than one; if $\lambda = \frac{1}{2}$, we have the standard case of a ship moving in the centreplane of the channel. It is assumed that the fluid was initially at rest, so the initial condition is

$$\phi^* = 0, \quad \zeta^* = 0 \quad (t^* = 0), \tag{7}$$

and the radiation condition is

$$\nabla^* \phi^* \to 0 \quad (x^* \to \pm \infty). \tag{8}$$

However, this latter condition must be modified in actual computation, specially for the downstream boundary, because the computational domain must be finite.

The pressure p^* is expressed by Bernoulli's equation,

$$\frac{p^*}{\rho^*} = -\left(\frac{\partial \phi^*}{\partial t^*} - U^* \frac{\partial \phi^*}{\partial x^*} + \tfrac{1}{2}|\nabla^* \phi^*|^2 + g^* z^* \right), \tag{9}$$

where ρ^* is the density of the fluid. The resulting forces and moments acting on the ship are given by

$$\left.\begin{aligned} F_x^* &= -\int_{S_w} p^* n_x \, \mathrm{d}S^*, \quad F_y^* = -\int_{S_w} p^* n_y \, \mathrm{d}S^*, \quad F_z^* = -\int_{S_w} p^* n_z \, \mathrm{d}S^*, \\ M_x^* &= -\int_{S_w} p^* (y^* n_z - z^* n_y) \, \mathrm{d}S^*, \quad M_y^* = -\int_{S_w} p^* (z^* n_x - x^* n_z) \, \mathrm{d}S^*, \\ M_z^* &= -\int_{S_w} p^* (x^* n_y - y^* n_x) \, \mathrm{d}S^*, \end{aligned}\right\} \tag{10}$$

where S_w denotes the actual wetted surface of the hull and $\boldsymbol{n} = (n_x, n_y, n_z)$ is the hull-outward normal unit vector on the surface S_w.

If the ship is free to heave and pitch, the motions in these two degrees of freedom are governed by the usual momentum equations. Assuming very slow motions, the inertial terms can be neglected so the momentum equations become simple equilibrium conditions. These are used to determine the running sinkage and trim at every timestep later on in this paper.

2.2. *Scale analysis*

We analyse the problem by the technique of matched asymptotic expansions. A key step in it is scale analysis, i.e. selection of small parameters and suitable scales. As the ship considered here is slender, a slenderness parameter is defined as

$$\delta = \frac{r_0^*}{l^*} \ll O(1), \quad r_0^* = (S_0^*)^{1/2}, \tag{11}$$

where S_0^* is the midship section area. If the ship generates only weakly nonlinear shallow-water waves, we have

$$\epsilon = \frac{A^*}{h^*}, \quad \mu = \frac{h^*}{L^*}, \quad O(\epsilon) = O(\mu^2) \ll O(1), \tag{12}$$

where A^* and L^* are the characteristic wave amplitude and length, respectively. A^* or ϵ can be determined by the ship hull boundary condition or by the matching condition to follow later. We select here $\epsilon = \mu^2$, which implies that both nonlinearity and dispersion of the wave will be included in the theory. However, this is not a serious restriction, because the theory can automatically adjust both effects and is valid even when the actual ratio ϵ/μ^2 is much greater or smaller than one, as long as both of them are small. Moreover, the ship length l^* may be of the same order as L^*.

Using the concept of matched asymptotics, we now divided the flow region into two parts, namely, near field and far field, meaning the fields near and far away from the ship, respectively. In the near field the typical lengthscale for transverse directions y and z is r_0^* and for longitudinal direction x it is l^*. On the other hand, in the far field the typical lengthscale for horizontal directions x and y is L^* and for vertical direction z it is h^*. The timescale, which is the same in both fields, must be determined by the shallow-water wave theory itself; in fact, it is of the order of the period of the wave generated by the ship or of the ship motion caused by the wave. Based on these scales, we can separately formulate equations with multiple-scale expansions for each field and then match them with each other asymptotically.

2.3. *The far field*

In the far field, upon introducing the normalization

$$\left.\begin{aligned} &\zeta = \frac{\zeta^*}{\epsilon h^*}, \quad \phi = \frac{\phi^*}{\epsilon^{1/2} h^* (g^* h)^{1/2}}, \quad x = \epsilon^{1/2} \frac{x^*}{h^*}, \quad y = \epsilon^{1/2} \frac{y^*}{h^*}, \quad z = \frac{z^*}{h^*}, \\ &t = \frac{\epsilon^{1/2} t^* (g^* h^*)^{1/2}}{h^*}, \quad F_{nh} = \frac{U^*}{(g^* h^*)^{1/2}}, \quad L^* = h^*/\epsilon^{1/2}, \quad p = \frac{p^*}{\rho^* g^* h^*}, \end{aligned}\right\} \tag{13}$$

and the following standard shallow-water expansion of (1)–(4) without considering the ship hull boundary condition (6),

$$\phi(x,y,z,t) = \phi_0(x,y,t) - \frac{\epsilon}{2!}(z+1)^2 \nabla^2 \phi_0(x,y,t) + \frac{\epsilon^2}{4!}(z+1)^4 \nabla^4 \phi_0(x,y,t) + \ldots, \tag{14}$$

in terms of the depth-averaged potential

$$\varphi(x,y,t) = \frac{1}{1+\epsilon\zeta} \int_{-1}^{\epsilon\zeta} \phi \, \mathrm{d}z = \phi_0 - \tfrac{1}{6}\epsilon(1+\epsilon\zeta)^2 \nabla^2 \phi_0 + O(\epsilon^2), \tag{15}$$

we obtain the Boussinesq equations,

$$\zeta_t - F_{nh}\,\zeta_x + \nabla\cdot[(1+\epsilon\zeta)\,\nabla\varphi] = 0, \tag{16}$$

$$\varphi_t - F_{nh}\,\varphi_x + \tfrac{1}{2}\epsilon|\nabla\varphi|^2 + \zeta = \tfrac{1}{3}\epsilon\nabla^2(\varphi_t - F_{nh}^{\prime}\,\varphi_x), \tag{17}$$

and the expression for pressure,

$$p = \epsilon\zeta - z + \tfrac{1}{2}\epsilon^2[(1+\epsilon\zeta)^2 - (1+z)^2]\,\nabla^2\zeta + O(\epsilon^3). \tag{18}$$

We further restrict the problem to the near-critical case, i.e. depth Froude number

$$F_{nh} = 1 + \alpha\epsilon, \quad \alpha \sim O(1). \tag{19}$$

In this case, the phase speed of waves generated is near the critical speed and the phase lines of the waves are almost perpendicular to the ship centreline, which means the waves fluctuate more slowly with time relative to an observer in the moving coordinate system and more gently in the y-direction than in the x-direction. So we renormalize

$$\tau = \epsilon t, \quad Y = \epsilon^{1/2} y, \tag{20}$$

and in terms of the new variables we get the simpler KP equation,

$$u_\tau - \alpha u_x + \tfrac{3}{2}uu_x + \tfrac{1}{6}F_{nh}\,u_{xxx} + \tfrac{1}{2}\varphi_{YY} = 0, \quad u = \varphi_x, \tag{21}$$

where u is also the first-order approximation of the free-surface elevation ζ. The channel sidewall boundary condition becomes

$$\varphi_Y = 0 \quad (Y = -\lambda\epsilon w^*/h^* \text{ and } (1-\lambda)\,\epsilon w^*/h^*). \tag{22}$$

The free-surface elevation itself is expressed as

$$\zeta = F_{nh}\,\varphi_x - \epsilon\varphi_\tau - \tfrac{1}{2}\epsilon\varphi_x^2 - \tfrac{1}{3}\epsilon F_{nh}\,\varphi_{xxx} + O(\epsilon^2). \tag{23}$$

2.4. *The near field*

In the near field, upon introducing the normalization

$$\left.\begin{aligned} \hat{x} &= \frac{x^*}{l^*}, \quad \hat{y} = \frac{y^*}{r_0^*}, \quad \hat{z} = \frac{z^*}{r_0^*}, \\ \hat{\phi}(\hat{x},\hat{y},\hat{z},\tau) &= \frac{\phi^*}{\epsilon^{1/2}h^*(g^*h^*)^{1/2}}, \quad \hat{\zeta}(\hat{x},\hat{y},\tau) = \frac{\zeta^*}{r_0^*}, \end{aligned}\right\} \tag{24}$$

we can get from (1)–(4) and (6),

$$\frac{\partial^2\hat{\phi}}{\partial\hat{y}^2} + \frac{\partial^2\hat{\phi}}{\partial\hat{z}^2} = -\delta^2\frac{\partial^2\hat{\phi}}{\partial\hat{x}^2} = -\epsilon\delta^2(l^*/h^*)^2\frac{\partial^2\varphi}{\partial x^2} + O(\epsilon^2\delta^2(l^*/h^*)^2), \tag{25}$$

$$\frac{\partial\hat{\phi}}{\partial\hat{z}} = O(\epsilon\delta) \quad (\hat{z} = \hat{\zeta}), \tag{26}$$

$$\frac{\partial\hat{\phi}}{\partial\hat{z}} = 0 \quad (\hat{z} = -\hat{h}), \tag{27}$$

$$\frac{\partial F}{\partial\hat{y}}\frac{\partial\hat{\phi}}{\partial\hat{y}} + \frac{\partial F}{\partial\hat{z}}\frac{\partial\hat{\phi}}{\partial\hat{z}} = \frac{S_0^*}{\epsilon^{1/2}l^*h^*}\frac{\partial F}{\partial\hat{x}}(F_{nh} - \epsilon\varphi_x|_{Y=0}) \quad (F = 0), \tag{28}$$

where $\hat{h} = h^*/r_0^*$. In (25) we have used the matching condition of longitudinal velocity $\partial\hat{\phi}/\partial\hat{x} = \epsilon^{1/2}l^*/h^*(\partial\varphi/\partial x)|_{Y\to 0} + O(\epsilon^{3/2}l^*/h^*)$ and continuity of wave elevation $\zeta|_{Y\to 0} = (r_0^*/\epsilon h^*)\,\hat{\zeta}|_{\hat{y}\to\infty}$ in advance. There is a formal solution for these linear equations,

$$\hat{\phi} = \frac{S_0^*}{\epsilon^{1/2}l^*h^*}(F_{nh} - \epsilon\varphi_x|_{Y=0})\,\psi_1(\hat{x},\hat{y},\hat{z}) - \epsilon\delta^2(l^*/h^*)^2\,\psi_2(\hat{x},\hat{y},\hat{z}) + \epsilon\frac{r_0^*}{h^*}V(\hat{x},\tau)\,\psi_3(\hat{x},\hat{y},\hat{z}) + f_0(\hat{x},\tau), \quad (29)$$

where V is the fluid velocity of cross-flow and f_0 a constant solution, both of which will be determined by matching with the far-field solution, ψ_1 and ψ_2 are particular solutions, and ψ_3 is a homogeneous solution, all of Laplace's equation, governed, respectively, by

$$\left.\begin{aligned} &\left(\frac{\partial^2}{\partial\hat{y}^2} + \frac{\partial^2}{\partial\hat{z}^2}\right)\psi_1 = 0, \\ &\frac{\partial F}{\partial\hat{y}}\frac{\partial\psi_1}{\partial\hat{y}} + \frac{\partial F}{\partial\hat{z}}\frac{\partial\psi_1}{\partial\hat{z}} = \frac{\partial F}{\partial\hat{x}}, \quad \text{on } F = 0; \quad \frac{\partial\psi_1}{\partial\hat{z}} = 0, \quad \text{on } \hat{z} = \hat{\zeta} \text{ and } -\hat{h}; \end{aligned}\right\} \quad (30)$$

$$\left.\begin{aligned} &\left(\frac{\partial^2}{\partial\hat{y}^2} + \frac{\partial^2}{\partial\hat{z}^2}\right)\psi_2 = \frac{\partial^2\varphi}{\partial x^2}, \\ &\frac{\partial F}{\partial\hat{y}}\frac{\partial\psi_2}{\partial\hat{y}} + \frac{\partial F}{\partial\hat{z}}\frac{\partial\psi_2}{\partial\hat{z}} = 0, \quad \text{on } F = 0; \quad \frac{\partial\psi_2}{\partial\hat{z}} = 0, \quad \text{on } \hat{z} = \hat{\zeta} \text{ and } -\hat{h}; \end{aligned}\right\} \quad (31)$$

$$\left.\begin{aligned} &\left(\frac{\partial^2}{\partial\hat{y}^2} + \frac{\partial^2}{\partial\hat{z}^2}\right)\psi_3 = 0, \\ &\frac{\partial F}{\partial\hat{y}}\frac{\partial\psi_3}{\partial\hat{y}} + \frac{\partial F}{\partial\hat{z}}\frac{\partial\psi_3}{\partial\hat{z}} = 0, \quad \text{on } F = 0; \quad \frac{\partial\psi_3}{\partial z} = 0, \quad \text{on } \hat{z} = \hat{\zeta} \text{ and } -\hat{h}. \end{aligned}\right\} \quad (32)$$

We do not need to find their exact solutions, but we must have their asymptotic nature in order to match them with the far field. By applying the law of mass conservation to a transverse fluid element surrounded by the hull surface, free surface, channel bottom and a control surface located far away from the ship but still within the near field, we have

$$\begin{aligned} &\lim_{\hat{y}\to\pm\infty}\left[\frac{S_0^*}{\epsilon^{1/2}l^*h^*}(F_{nh} - \epsilon u_0)\frac{\partial\psi_1(\hat{x},\hat{y},\hat{z})}{\partial\hat{y}} - \epsilon\delta^2(l^*/h^*)^2\frac{\partial\psi_2(\hat{x},\hat{y},\hat{z})}{\partial\hat{y}}\right] \\ &= \mp\frac{1}{2}\frac{r_0^{*3}}{\epsilon^{1/2}l^*h^{*2}(1+\epsilon u_0)}\left[\frac{\mathrm{d}\hat{S}}{\mathrm{d}\hat{x}}(F_{nh} - \epsilon u_0) + \epsilon(2\hat{h}|\hat{y}| - \hat{S})\frac{\mathrm{d}u_0}{\mathrm{d}\hat{x}}\right] \\ &= \mp\frac{1}{2}\frac{r_0^{*3}}{\epsilon^{1/2}l^*h^{*2}(1+\epsilon u_0)}\left\{\frac{\mathrm{d}}{\mathrm{d}\hat{x}}\left[\hat{S}(F_{nh} - \epsilon u_0)\right] + 2\epsilon\hat{h}|\hat{y}|\frac{\mathrm{d}u_0}{\mathrm{d}\hat{x}}\right\}, \end{aligned} \quad (33)$$

where $u_0 = u|_{Y=0} = \varphi_x|_{Y=0}$ and $\hat{S}(\hat{x},t) = S^*(\hat{x},t)/S_0^*$ for $-\frac{1}{2} \leqslant \hat{x} \leqslant \frac{1}{2}$ is the actual time-dependent underwater cross-sectional area of the ship. Further, for the cross-flow we obtain analytically

$$\lim_{\hat{y}\to\pm\infty}\psi_3(\hat{y},\hat{z}) = \hat{y} \pm C(\hat{x}), \quad (34)$$

where $C(\hat{x})$ is called the blockage coefficient of such a section and can be calculated,

e.g. by a boundary-element method (Newman 1969; Taylor 1973). However, for the symmetric case, we need not calculate it because there is no cross-flow at all, i.e. $V = 0$ in (29). Substituting (33) and (34) into (29) yields

$$\lim_{\hat{y}\to\pm\infty}\hat{\phi} = -\frac{1}{2}\frac{r_0^{*3}}{\epsilon^{1/2}l^*h^{*2}}\frac{|\hat{y}|}{(1+\epsilon u_0)}\left\{\frac{\mathrm{d}}{\mathrm{d}\hat{x}}[\hat{S}(F_{nh}-\epsilon u_0)]+\epsilon\hat{h}|\hat{y}|\frac{\mathrm{d}u_0}{\mathrm{d}\hat{x}}\right\}$$

$$+\epsilon\frac{r_0^*}{h^*}V(\hat{x},\tau)[\hat{y}\pm C(\hat{x},\tau)]+f_0(\hat{x},\tau). \quad (35)$$

Invoking (9), the pressure distribution in the near field can be expressed with sufficient precision as

$$p = -\epsilon\hat{\phi}_\tau - \tfrac{1}{2}\epsilon(h^*/l^*)^2\hat{\phi}_{\hat{x}}^2 - \frac{\epsilon h^{*2}}{2S_0^*}\hat{\phi}_{\hat{y}}^2 - \frac{\epsilon h^{*2}}{2S_0^*}\hat{\phi}_{\hat{z}}^2 + \epsilon^{1/2}(h^*/l^*)F_{nh}\hat{\phi}_{\hat{x}} - z + O(\epsilon^3). \quad (36)$$

From the estimate,

$$\hat{\Phi}_{\hat{y}} \sim \hat{\phi}_{\hat{z}} \sim O\left(\frac{S_0^*}{\epsilon^{1/2}l^*h^*}\right) \sim O(\epsilon),$$

we can see that $\hat{\phi}_{\hat{y}}$ and $\hat{\phi}_{\hat{z}}$ are small and of same order as ϵ. So if h^{*2}/S_0^* is not large, the terms involving $\hat{\phi}_{\hat{y}}$ and $\hat{\phi}_{\hat{z}}$ can be omitted in the above pressure expression.

2.5. *Matching conditions*

According to the principle of matched asymptotics, i.e. the expansion of the far field to the near field must be equal to the expansion of the near field to the far field, we establish the matching conditions from (35) as follows:

$$\zeta|_{Y\to 0} = (r_0^*/\epsilon h)\hat{\zeta}|_{\hat{y}\to\infty}, \quad \phi_x|_{Y\to 0} = \frac{l^*}{h^*}\epsilon^{1/2}\hat{\phi}_{\hat{x}}|_{\hat{y}\to\infty}, \quad (37)$$

$$\epsilon\frac{\partial\varphi}{\partial Y}\bigg|_{Y\to 0^\pm} = \mp\frac{1}{2}\frac{S_0^*}{\epsilon^{1/2}l^*h^*(1+\epsilon u_0)}\frac{\mathrm{d}}{\mathrm{d}\hat{x}}[\hat{S}(F_{nh}-\epsilon u_0)]+\epsilon V, \quad (38)$$

$$\hat{\phi}|_{Y\to 0^+} - \hat{\phi}|_{Y\to 0^-} = 2VC\epsilon\frac{r_0^*}{h^*}, \quad (39)$$

$$\hat{\phi}|_{Y\to 0^+} + \hat{\phi}|_{Y\to 0^-} = 2f_0. \quad (40)$$

Substituting V from (39) into (38) will yield a single boundary condition for the far-field KP equation. However, if the problem is symmetric about the x-axis, we can simply set $V = 0$ in (38). Owing to normalization of (38) we have an important relation,

$$\epsilon^{3/2} = \frac{S_0^*}{l^*h^*} = \delta^2\frac{l^*}{h^*}, \quad (41)$$

which means that ϵ is not only related to the slenderness δ but also to the ratio of ship length to water depth. Compared with Choi & Mei (1989) who assumed $r_0^*/h^* = O(\mu)$, no such restriction is introduced here, i.e. r_0^*/h^* may be from $O(\epsilon^{1/2})$ up to $O(1)$. Mei (1976) extensively discussed different combinations of smallness parameters of waves and ships (or struts). The case of $O(\epsilon^{1/2}) \leqslant r_0^*/h^* \leqslant O(1)$ corresponds to his cases from medium-amplitude waves to large-amplitude waves or in his words to a 'thick'

strut. This is a very practical range for many types of ship such as aircraft carriers, passenger ships and fast cargo ships which can attain near-critical speeds and even exceed the critical speed.

As a consequence of our higher-order approximation in the near field, the instantaneous underwater cross-sectional area $\hat{S}$ should include effects of running sinkage, trim and wave elevation. If the ship sidewalls are nearly vertical or sinkage, trim and wave elevation are relatively small, the required cross-sectional area can be expressed approximately as

$$\hat{S}(\hat{x},\tau) = S_s(\hat{x}) + \frac{b_0^* h^*}{S_0^*} b(\hat{x}) \left[\frac{l^*}{h^*} (s(\tau) - \hat{x}\theta(\tau)) + \epsilon\zeta_0(\hat{x},\tau) \right], \tag{42}$$

where s and θ denote sinkage and trim, ζ_0 denotes wave elevation at ship sidewall, and $S_s(\hat{x})$ is the still-water cross-sectional area distribution.

It is evident that (38) involves two types of nonlinearity: one of relative order amplitude/draught, say, that is contained in $\hat{S}$ and the other of order amplitude/depth appearing through the factor ϵu_0. The first nonlinearity is stronger than the second, which is of the same order as that included in the KP equation in the far field. Equation (38) can be reduced to the classic matching condition $(\partial\varphi/\partial Y)|_{Y\to 0^{\pm}} = \mp\frac{1}{2}F_{nh}(\mathrm{d}/\mathrm{d}\hat{x})S_s$ by neglecting terms with factor ϵ and putting $V = 0$. This was widely used in previous applications of slender-body theory. It is clear that this classic approach does not account for the full interaction between the near and far fields. It includes the effect of the body (near field) on the waves (far field), but not that of the waves on the body. The present matching condition (38) does reflect such interaction. The far-field solution is incorporated into the near-field solution (38) and (42) so that the waves or flows generated by each section in the near-field will interact mutually through the far-field solution.

We cannot extend the calculation region wide enough downstream to ensure that the water there is still undisturbed but we can move the downstream boundary far enough so that the waves there are almost propagating in the negative x-direction and are not as strong as those around the ship. Hence, an outward radiation condition can be imposed there,

$$\frac{\partial u}{\partial \tau} - C_{-\infty}\frac{\partial u}{\partial x} = 0 \quad (C_{-\infty} > 0). \tag{43}$$

Here $C_{-\infty}$ is the phase speed of downstream waves which, exactly speaking, is a function of Y and time, to be determined approximately by the numerical procedure itself. However, theoretically $C_{-\infty} \to 0$ as $\tau \to +\infty$, as the wave in the wake will tend to become stationary in the moving frame. On the other hand, we can select the upstream region big enough so that the condition of no disturbance is still valid at the boundary.

$$\varphi_x = 0, \quad \varphi = 0 \quad (x \to +\infty). \tag{44}$$

From (36) with (37) and (23) the pressure on the ship hull can be expressed approximately as,

$$p = \epsilon\zeta|_{Y=0} - z + O(\epsilon^2), \tag{45}$$

in conformity with (18).

2.6. *Handling a blunt bow or stern*

We have seen in §2.4 that our slender-body theory in the near field even includes certain three-dimensional effects, so the requirement of slenderness is quite weak. However, if the bow or stern of the ship is not sharp enough, we must modify the theory. Based on

the idea that a point source at the bow or a sink at the stern will affect the far field in all directions rather than in the transverse direction only as in (38), we can move the source singularity at a blunt bow or stern from the matching condition (38) to the forcing term in the governing KP equation heuristically, yielding

$$u_\tau - \alpha u_x + \tfrac{3}{2}uu_x + \tfrac{1}{6}F_{nh}\,u_{xxx} + \tfrac{1}{2}\varphi_{YY} = \tfrac{1}{2}Q\delta(x-x_0)\,\delta(Y), \tag{46}$$

$$Q = -\int_{x_0}^{x_0-\delta_1} \frac{1}{1+\epsilon u_0}\frac{\mathrm{d}}{\mathrm{d}\hat{x}}[\hat{S}(F_{nh}-\epsilon u_0)]\frac{\epsilon^{1/2}l^*}{h^*}\,\mathrm{d}\hat{x}, \tag{47}$$

$$\left.\frac{\partial\varphi}{\partial Y}\right|_{Y=0^\pm} = \mp\frac{1}{2}\frac{1}{1+\epsilon u_0}\frac{\mathrm{d}}{\mathrm{d}\hat{x}}[\hat{S}(F_{nh}-\epsilon u_0)] + V \quad (-x_0 \leqslant \hat{x} < x_0-\delta_1), \tag{48}$$

where $\delta(x)$ is Dirac function, x_0 is x-coordinate at the bow and δ_1 is a small parameter that is a measure of bluntness of the bow. We see that in (47) only the bow singularity is included. Although the stern singularity could also be included in the same way, we neglect it because in real flow the viscous wake will damp or distort the effect of the stern singularity. For a not very blunt but no longer sharp bow, we can separate a fraction of Q from (38) to add into (21), and still retain the rest in (38). The fraction is related to the bluntness of the bow but it is selected somewhat artificially. We use this technique only for the Series 60, $C_B = 0.8$ model. There is no difficulty in realizing this process of dealing with a blunt bow in the numerical technique implemented.

2.7. *Hydrodynamic forces on the ship*

For the longitudinal and vertical forces F_x^*, F_z^* and moment M_y^*, we can integrate (10) directly by substituting (45) into it. Conventionally, instead of F_x^*, F_z^* and M_y^*, we want to know wave resistance R_w^*, lift force F_L^* and trim moment M_T^* about the centre of gravity G with defined bow-up positive direction, which are written as

$$R_w^* = -F_x^*, \quad F_L^* = F_z^* - m^*g^*, \quad M_T^* = -M_y^* - F_z^*\,x_G^* + F_x^*\,z_G^*, \tag{49}$$

where m^* is the mass of the ship, and x_G^* and z_G^* are x^* and z^* coordinates of the centre of gravity G in $Ox^*y^*z^*$. They are non-dimensionalized as

$$R_w = \frac{R_w^*}{m^*g^*}, \quad F_L = \frac{F_L^*}{m^*g^*}, \quad M_T = \frac{M_T^*}{m^*g^*l^*}. \tag{50}$$

Carefully calculating the expression for R_w, we get

$$\begin{aligned} R_w &= \frac{h^*}{l^*C_P}\int_{S_w}(\epsilon\zeta_0 - z)\,n_x\,\mathrm{d}S \\ &= \frac{h^*}{l^*C_P}\left[\int_{-1/2}^{1/2}\epsilon\zeta_0\left(\int_{l_g} n_x\,\mathrm{d}l\right)\mathrm{d}\hat{x} - \int_{S_w} zn_x\,\mathrm{d}S\right] \end{aligned} \tag{51}$$

where

$$\int_{l_g} n_x\,\mathrm{d}l = -\left\{\frac{\mathrm{d}}{\mathrm{d}\hat{x}}\left[S_s + \frac{b_0^*l^*}{S_0^*}b(\hat{x})(s-\hat{x}\theta)\right] + \frac{b_0^*h^*}{S_0^*}\epsilon\zeta_0\frac{\mathrm{d}b}{\mathrm{d}\hat{x}}\right\}, \tag{52}$$

$$-\int_{S_w} zn_x\,\mathrm{d}S = \int_{-1/2}^{1/2}\frac{\epsilon^2h^*b_0^*}{2S_0^*}\zeta_0^2\frac{\mathrm{d}b}{\mathrm{d}\hat{x}}\,\mathrm{d}\hat{x}. \tag{53}$$

Here, $C_P = V_0^*/S_0^* l^*$ is the longitudinal prismatic coefficient, V_0^* is static displacement volume of the ship, $\zeta_0 = \zeta|_{Y=0}$, l_g is the wetted girth of each cross-section, $s = s^*/l^*$ is sinkage, and θ is the trim angle. We can also obtain expressions for lift force and trim moment,

$$F_L = \frac{\epsilon h^*}{C_B d^*} \int_{-1/2}^{1/2} \left[\zeta + \frac{l^*}{\epsilon h^*}(s - \hat{x}\theta) \right] b(\hat{x})\, \mathrm{d}\hat{x}, \tag{54}$$

$$M_T = \frac{\epsilon h^*}{C_B d^*} \int_{-1/2}^{1/2} \left[\zeta + \frac{l^*}{\epsilon h^*}(s - \hat{x}\theta) \right] b(\hat{x})(-\hat{x})\, \mathrm{d}\hat{x} - F_L \frac{x_G^*}{l^*}, \tag{55}$$

where the contribution of forces in the x-direction to the trim moment is neglected and $C_B = V_0^*/(l^* b_0^* d^*)$ is the block coefficient of the ship.

2.8. *Sinkage and trim*

For a ship free to heave and pitch, assuming sinkage and trim to vary slowly with time the inertial force and moment are accordingly small. So we can omit them and then the quasi-steady hydrodynamic equilibrium requires just $F_L = 0$ and $M_T = 0$, i.e. zero lift-force and trim-moment, which yields

$$\int_{-1/2}^{1/2} \left[\zeta + \frac{l^*}{\epsilon h^*}(s - \hat{x}\theta) \right] b(\hat{x})\, \mathrm{d}\hat{x} = 0, \tag{56}$$

$$\int_{-1/2}^{1/2} \left[\zeta + \frac{l^*}{\epsilon h^*}(s - \hat{x}\theta) \right] b(\hat{x})(-\hat{x})\, \mathrm{d}\hat{x} = 0. \tag{57}$$

The above two equations constitute linear algebraic equations for s and θ and are easy to solve.

For the lateral force and yaw moment, we cannot use the mean pressure expression (45), but we could use the law of conservation of momentum in lateral direction in the near field to get them. Because we only treat the symmetric case in the following numerical examples, we do not pursue this matter here.

3. Finite difference schemes for the KP equation

Finding a numerical technique for solving the KP equation (2) is not a trivial task. We present here a set of efficient and precise finite-difference schemes using the fractional step algorithm (Yanenko 1971). A similar technique was successfully applied by Chen & Liu (1988) to solve the KP equation for the problem of diffraction of a solitary wave by a thin wedge.

Define a net function as

$$\left.\begin{aligned} \varphi_{i,j}^n &= \varphi(i\Delta x, (j - \mathrm{sign}\,(j))\Delta Y, n\Delta\tau), \\ \text{for} \qquad i &= -I_{min}, \ldots, I_{max}, \quad j = -J_{min}, \ldots, J_{max}+1, \quad n = 0, \ldots, N. \end{aligned}\right\} \tag{58}$$

where

$$\text{sign}(j) = \begin{cases} 0, & j \leqslant 0, \\ 1, & j > 0, \end{cases}$$

$\varphi(i,0,n) = \varphi|_{Y=0^-}$ and $\varphi(i,1,n) = \varphi|_{Y=0^+}$ at the ship location $i = -I_{ship}, \ldots, I_{ship}$, elsewhere $\varphi(i,0,n) = \varphi(i,1,n) = \varphi|_{Y=0}$. The other variables, e.g. u, also have similarly defined net functions.

The KP equation (21) is solved numerically by a fractional step algorithm which separates (21) into two parts, $u_\tau - \alpha u_x + \frac{3}{2} u u_x + \frac{1}{6} F_{nh} u_{xxx} = 0$ and $u_\tau + \frac{1}{2}\varphi_{YY} = 0$, at two half-steps. For each of them, the Crank–Nicolson type schemes are constructed, which are implicit, energy conservative and of second-order precision. For the first half-step, we have

$$\begin{aligned}
&(\tilde{u}_i - u_i^n)/\Delta\tau - \frac{\alpha}{4\Delta x}[(\tilde{u}_{i+1} - \tilde{u}_{i-1}) + (u_{i+1}^n - u_{i-1}^n)] \\
&+ \frac{1}{8\Delta x}[(\tilde{u}_{i+1} + \tilde{u}_i + \tilde{u}_{i-1})(u_{i+1}^n - u_{i-1}^n) + (u_{i+1}^n + u_i^n + u_{i-1}^n)(\tilde{u}_{i+1} - \tilde{u}_{i-1})] \\
&+ \frac{F_{nh}}{24(\Delta x)^3}[(\tilde{u}_{i+2} - 2\tilde{u}_{i+1} + 2\tilde{u}_{i-1} - \tilde{u}_{i-2}) \\
&+ (u_{i+2}^n - 2u_{i+1}^n + 2u_{i-1}^n - u_{i-2}^n)] = 0 \quad \text{for} \quad i = -I_{min} + 2, \ldots, I_{max} - 2, \qquad (59)
\end{aligned}$$

where subscript j is omitted above as well as in the following formulae in this paragraph for the sake of convenience, and $\tilde{u}$ is an intermediate value of u. The above scheme needs two-line complementary boundary conditions at the upstream and downstream ends. So it needs to be modified at the first inner line of the downstream end and must also be calculated together with the upstream and downstream boundary conditions, i.e. radiation conditions at both ends of (43) and (44). Thus we put

$$\begin{aligned}
&(\tilde{u}_i - u_i^n)/\Delta\tau - \frac{\alpha}{4\Delta x}[(\tilde{u}_{i+1} - \tilde{u}_{i-1}) + (u_{i+1}^n - u_{i-1}^n)] \\
&+ \frac{1}{8\Delta x}[(\tilde{u}_{i+1} + \tilde{u}_i + \tilde{u}_{i-1})(u_{i+1}^n - u_{i-1}^n) + (u_{i+1}^n + u_i^n + u_{i-1}^n)(\tilde{u}_{i+1} - \tilde{u}_{i-1})] \\
&+ \frac{F_{nh}}{12(\Delta x)^3}[(\tilde{u}_{i+2} - 3\tilde{u}_{i+1} + 3\tilde{u}_i - \tilde{u}_{i-1}) \\
&+ (u_{i+2}^n - 3u_{i+1}^n + 3u_i^n - u_{i-1}^n)] = 0 \quad (i = -I_{min} + 1), \qquad (60)
\end{aligned}$$

$$(\tilde{u}_i - u_i^n)/\Delta\tau - \frac{C_{-\infty}}{\Delta x}(u_{i+1}^n - u_i^n) = 0 \quad (i = -I_{min}), \qquad (61)$$

$$\tilde{u}_i = 0 \quad (i = I_{max}, I_{max} - 1). \qquad (62)$$

For the other half-step, the scheme is constructed as,

$$\begin{aligned}
&(u_{i,j}^{n+1} - \tilde{u}_{i,j})/\Delta\tau + \frac{\Delta x}{4(\Delta Y)^2}[(\Phi_{i+1,j+1}^{n+1} - 2\Phi_{i+1,j}^{n+1} + \Phi_{i+1,j-1}^{n+1}) \\
&- \tfrac{1}{2}(u_{i,j+1}^{n+1} - 2u_{i,j}^{n+1} + u_{i,j-1}^{n+1})] + \frac{1}{4(\Delta Y)^2}[\tilde{\varphi}_{i,j+1} - 2\tilde{\varphi}_{i,j} + \tilde{\varphi}_{i,j-1}] = 0 \quad (j \neq 0, 1), \qquad (63)
\end{aligned}$$

where

$$\Phi^n_{i,j} = -\sum_{i=i}^{I_{max}} u^n_{i,j} = \Phi^n_{i+1,j} - u^n_{i,j},$$

$$\tilde{\varphi}_{i,j} = -\sum_{i=i}^{I_{max}} \tfrac{1}{2}(\tilde{u}_{i+1,j} + \tilde{u}_{i,j})\,\Delta x.$$

The scheme (63) should be calculated together with the boundary conditions at the cut of the ship location and the sidewalls of the channel. Owing to the matching conditions (38) and (39) at the cut of the ship location ($-I_{ship} \leqslant i \leqslant I_{ship}$), we get

$$(u^{n+1}_{i,j} - \tilde{u}_{i,j})/\Delta\tau + \frac{\Delta x}{4(\Delta Y)^2}\left[2\Phi^{n+1}_{i+1,j-1} - 2\Phi^{n+1}_{i+1,j} + \frac{h^*\Delta Y}{\epsilon C_{i+1} b^*}(\Phi^{n+1}_{i+1,j+1} - \Phi^{n+1}_{i+1,j})\right]$$
$$+ \frac{(1+\epsilon\tilde{u}_0)^{-1}\Delta[\hat{S}_i(F_{nh} - \epsilon\tilde{u}_0)]}{2\Delta Y\,\Delta\hat{x}} - \frac{\Delta x}{8(\Delta Y)^2}\left[2u^{n+1}_{i,j-1} - 2u^{n+1}_{i,j} + \frac{h^*\Delta Y}{\epsilon C_i b^*}(u^{n+1}_{i,j+1} - 2u^{n+1}_{i,j})\right]$$
$$+ \frac{1}{4(\Delta Y)^2}\left[2\tilde{\varphi}_{i,j-1} - 2\tilde{\varphi}_{i,j} + \frac{h^*\Delta Y}{\epsilon C_i b^*}(\tilde{\varphi}_{i,j+1} - 2\tilde{\varphi}_{i,j})\right] = 0 \quad (j = 0), \tag{64}$$

$$(u^{n+1}_{i,j} - \tilde{u}_{i,j})/\Delta\tau + \frac{\Delta x}{4(\Delta Y)^2}\left[2\Phi^{n+1}_{i+1,j+1} - 2\Phi^{n+1}_{i+1,j} - \frac{h^*\Delta Y}{\epsilon C_{i+1} b^*}(\Phi^{n+1}_{i+1,j} - \Phi^{n+1}_{i+1,j-1})\right]$$
$$+ \frac{(1+\epsilon\tilde{u}_0)^{-1}\Delta[\hat{S}_i(F_{nh} - \epsilon\tilde{u}_0)]}{2\Delta Y\,\Delta\hat{x}} - \frac{\Delta x}{8(\Delta Y)^2}\left[2u^{n+1}_{i,j+1} - 2u^{n+1}_{i,j} - \frac{h^*\Delta Y}{\epsilon C_i b^*}(u^{n+1}_{i,j} - 2u^{n+1}_{i,j-1})\right]$$
$$+ \frac{1}{4(\Delta Y)^2}\left[2\tilde{\varphi}_{i,j+1} - 2\tilde{\varphi}_{i,j} - \frac{h^*\Delta Y}{\epsilon C_i b^*}(\tilde{\varphi}_{i,j} - 2\tilde{\varphi}_{i,j-1})\right] = 0 \quad (j = 1), \tag{65}$$

and for the channel sidewall condition (22) we have simply

$$u^{n+1}_{i,j+1} = u^{n+1}_{i,j-1} \quad (j = -J_{min}, J_{max} + 1). \tag{66}$$

The scheme (63) with (64), (65) and (66) proceeds in the sequence of decreasing i, i.e. from the upstream end $i = I_{max}$ to the downstream end $i = -I_{min}$. It is easy to see that (59)+(63) is consistent with the original KP equation (21) to second-order precision in $\Delta\tau$.

The numerical procedure is carried out step by step with increasing timestep n. When $n = 0$, all u and φ are zero as determined by initial condition (7). At step $n+1$, $u^n_{i,j}$ is already known and the unknown $u^{n+1}_{i,j}$ is obtained in two half-steps. In the first half-step, for any j, (59) along with boundary conditions (60), (61) and (62) constitute linear algebraic equations of a quin-diagonal matrix for the intermediate value $\tilde{u}_{i,j}$, which can be solved by an extended double sweep method for the quin-diagonal matrix. In the other half-step, for any i, (63) along with boundary conditions (64), (65) and (66) constitute linear algebraic equations of a tri-diagonal matrix for $u^{n+1}_{i,j}$, which can be solved by a double sweep method for the tri-diagonal matrix. Repeating the above procedure, all $u^n_{i,j}$ $(n = 0, \ldots, N)$ are determined.

The nonlinearity of the equation and the boundary conditions will generally cause numerical instability. A rigorous analysis of this kind of instability is almost impossible. So we construct and use this set of schemes in the sense of an empirical numerical technique. In order to overcome the instability, we add very small artificial viscous effects of type νu_{xx} and νu_{YY} in the radiation conditions at the ends and the matching conditions at the ship location. Even then, we still need to select suitable values of $\Delta\tau$, Δx and ΔY to avoid instability.

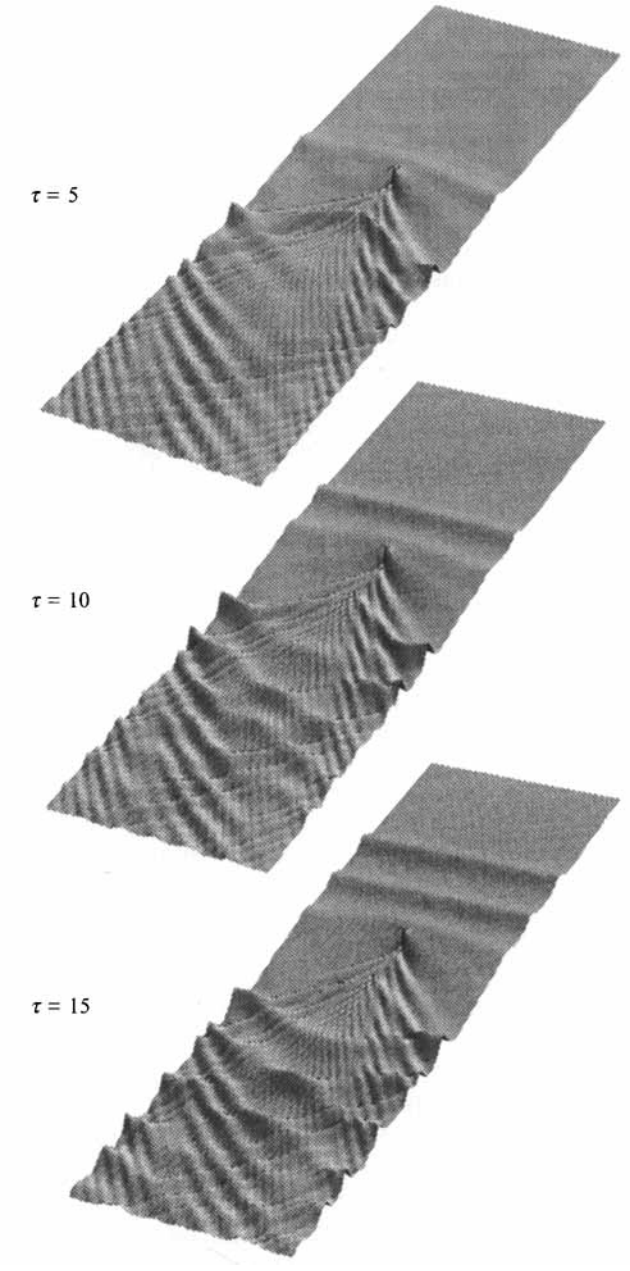

FIGURE 1. Wave evolution for Series 60 model at the critical speed in case $w^* = 4.88$ m where the viewed horizontal area is 17.1×4.88 m^2 and the vertical scale is exaggerated 5 times.

In the following numerical examples, we set $\Delta\tau = 0.01, \Delta x = \epsilon^{1/2} l^*/(h^* 2 I_{ship})$, $I_{ship} = 10$–$20, \Delta Y = \epsilon w^*/h^*(J_{min} + J_{max})$, the radiation boundary is located far away from the ship at a distance of 20–40 times the ship length, and ν is about 0.05. For example, in the calculation of Series 60, $C_B = 0.8$ model for the case of Ertekin *et al.* (1984), we set $\Delta\tau = 0.01$, $\Delta x = 0.107229$ and $\Delta Y = 0.091072$. Choi & Mei (1989) and Choi *et al.* (1990) used an explicit scheme of Katsis & Akylas (1987), they selected $\Delta\tau = 0.00002$, $\Delta x = 0.1$ and $\Delta Y = 0.1$ for the same case. Although our schemes are

(*a*) Amplitude

A^*/h^*		$w^* = 1.22$ m	$w^* = 2.44$ m	$w^* = 4.88$ m
$F_{nh} = 0.9$	Choi's KP	0.480	0.315	0.202
	Our KP	0.403	0.274	0.163
	Exp	0.367	0.273	0.143
$F_{nh} = 1.0$	Choi's KP	0.623	0.445	0.322
	Our KP	0.580	0.436	0.319
	Exp	0.551	0.438	0.303
$F_{nh} = 1.1$	Choi's KP	0.785	0.625	0.490
	Our KP	0.769	0.624	0.496
	Exp	0.608	0.585	0.480

(*b*) Period

U^*T^*/h^*		$w^* = 1.22$ m	$w^* = 2.44$ m	$w^* = 4.88$ m
$F_{nh} = 0.9$	Choi's KP	20.04	31.83	41.26
	Our KP	25.16	38.57	54.00
	Exp	32.70	48.10	65.10
$F_{nh} = 1.0$	Choi's KP	24.89	39.29	60.26
	Our KP	29.54	46.02	71.74
	Exp	37.80	49.80	85.20
$F_{nh} = 1.1$	Choi's KP	33.14	54.75	90.78
	Our KP	35.69	59.47	96.46
	Exp	39.00	50.11	103.60

TABLE 1. The amplitude of the first soliton and the generation period between the first two solitons for the Series 60 model.

implicit, the numerical task at each timestep is not much larger than that in explicit schemes. Because we have reduced the problem to two diagonal-matrix equations with the fractional step algorithm, the task of solving the equations is of the same order of magnitude as an explicit calculation. Even if we assume that our task at each step takes 50 times as much CPU time as Choi & Mei (1989), our numerical technique is still 10 times more efficient than theirs.

4. Numerical examples

We have calculated three ship models: Series 60, $C_B = 0.8$ model, Taylor Standard Series model and Wigley mathematical model in the speed range of $F_{nh} = 0.88$–1.12 and all are symmetric cases. All examples are compared with existing experimental results and the cases of Series 60 model and Wigley model are also compared with previous calculations.

4.1. *Series 60 model*

To investigate the dynamic nature of solitary waves generated in front of the ship, we calculate the same cases as in the experiments of Ertekin *et al.* (1985) and the calculations of Choi *et al.* (1990), in which the towing mode was fixed and a Series 60 model with $C_B = 0.8$ was chosen. Its length, beam and draft are 1.52 m, 0.23 m and 0.075 m, respectively. The water depth is 0.15 m and the three tank widths are 1.22 m, 2.44 m and 4.88 m. First, we show perspective views of the wave pattern for the case of tank width 4.88 m and $F_{nh} = 1$ in figure 1 where the vertical displacement is exaggerated 5 times for clarity. Around the bow of the ship, the local wave builds up, forms a one-dimensional solitary wave and is emitted in front of the bow, going a bit faster than the ship. Further, the process is repeated periodically and the solitary waves

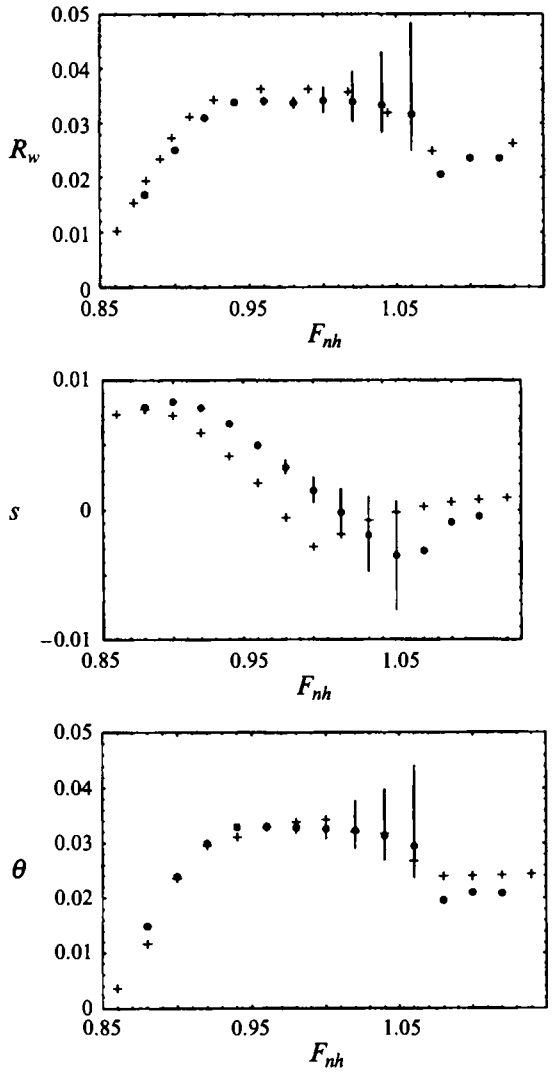

FIGURE 2. Calculated wave resistance, sinkage and trim as compared with Graff's experiments for $h^*/l^* = 0.125$: ●, average calculated values; |, range of variation between minimum and maximum in the calculations; +, measured values.

are generated continuously, which makes other variables, e.g. the hydrodynamic forces on the ship, also vary periodically with time.

The amplitude of the first soliton and the generation period between the first two solitons are listed in table 1 together with calculated results of the KP model of Choi *et al.* (1990) and experimental measurements of Ertekin *et al.* (1984). Our values in almost all cases are closer to the experimental ones than Choi's. It is not surprising because the near-field approximation in our theory includes second-order terms that were omitted in Choi *et al.* (1990). Besides, we use the technique described in §2.6 to deal explicitly with the blunt bow, whereas portions of the bow and stern were slightly modified by a parabolic distribution in Choi *et al.* (1990). Since Series 60, $C_B = 0.8$ hullform is not very blunt at the bow, we separate one half of the source strength Q generated in the first discrete interval at the bow from (38) and enter it into (21) to get

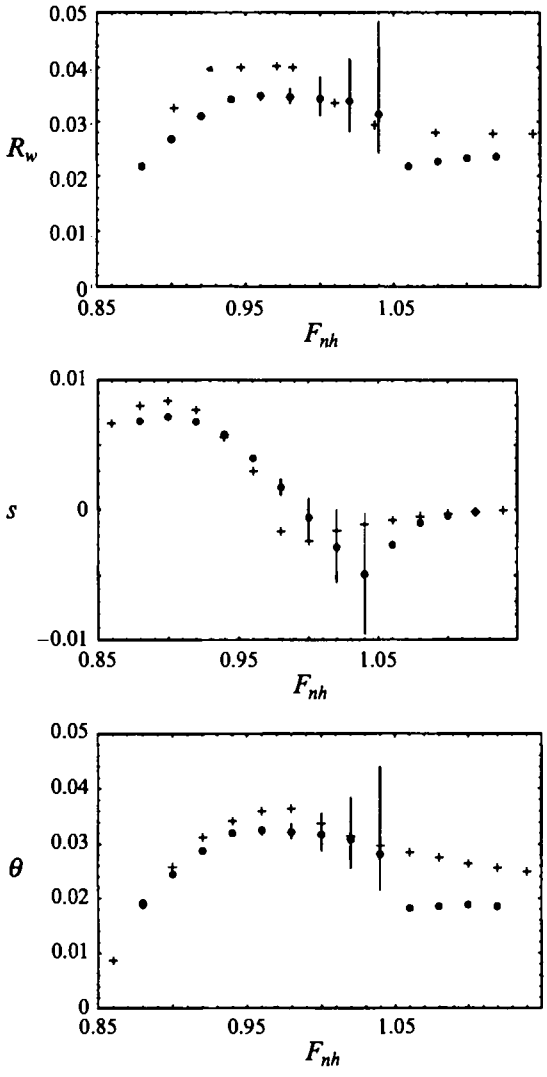

FIGURE 3. Calculated wave resistance, sinkage and trim as compared with Graff's experiments for $h^*/l^* = 0.167$. Key as figure 2.

(46); the other half remains in (38). Numerical experiments show that the effect of the divided bow source on wave resistance, period and amplitude of the solitons is within 5%, but it affects the computational procedure in the favourable direction of numerical stability. We have also done calculations omitting the higher-order terms in boundary conditions (38) and without special handling of the bow, which means using the same boundary conditions as Choi *et al.* (1990) to solve the KP equation but by a different numerical method, and confirmed their results very closely. Since the amplitude of the solitons exceeds half the water depth, the KP equation is on the margin of its validity. One could possibly resort to shallow-water wave equations including even higher-order nonlinearities in the far field. Such effects have been studied, e.g. by Ertekin *et al.* (1986) based on the Green–Naghdi equations and by Tomasson & Melville (1991) using a suitable numerical technique to allow a cubic nonlinearity with application also to the two-fluid-layer flow problem.

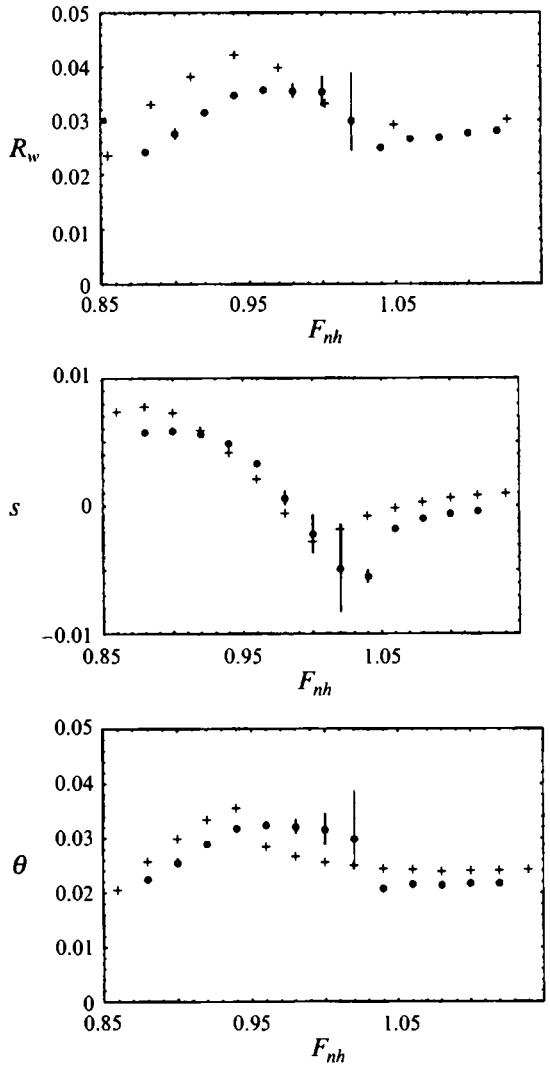

FIGURE 4. Calculated wave resistance, sinkage and trim as compared with Graff's experiments for $h^*/l^* = 0.208$. Key as figure 2.

We can, of course, also get the wave resistance, lift force and trim moment for these cases, but we omit them here for the sake of brevity and because there are no corresponding experimental results to compare with. The reader is referred to the calculated results in figures 6–8 of Choi *et al.* (1990).

4.2. *Taylor standard series model*

The Taylor standard series model of $C_P = 0.64$ with length $l^* = 3$ m, beam $b^* = 0.27845$ m and draft $d^* = 0.0928$ m was used in the systematic shallow-water model experiments by Graff *et al.* (1964) in the Duisburg shallow water towing tank. The tank was 10.1 m wide and the water depth was set at six values $h^*/l^* = 0.333$, 0.25, 0.208, 0.167, 0.125 and 0.05 in the experiments. The ship model was free to heave and pitch. In our calculation, the model and the channel geometry is chosen to be same as in Graff

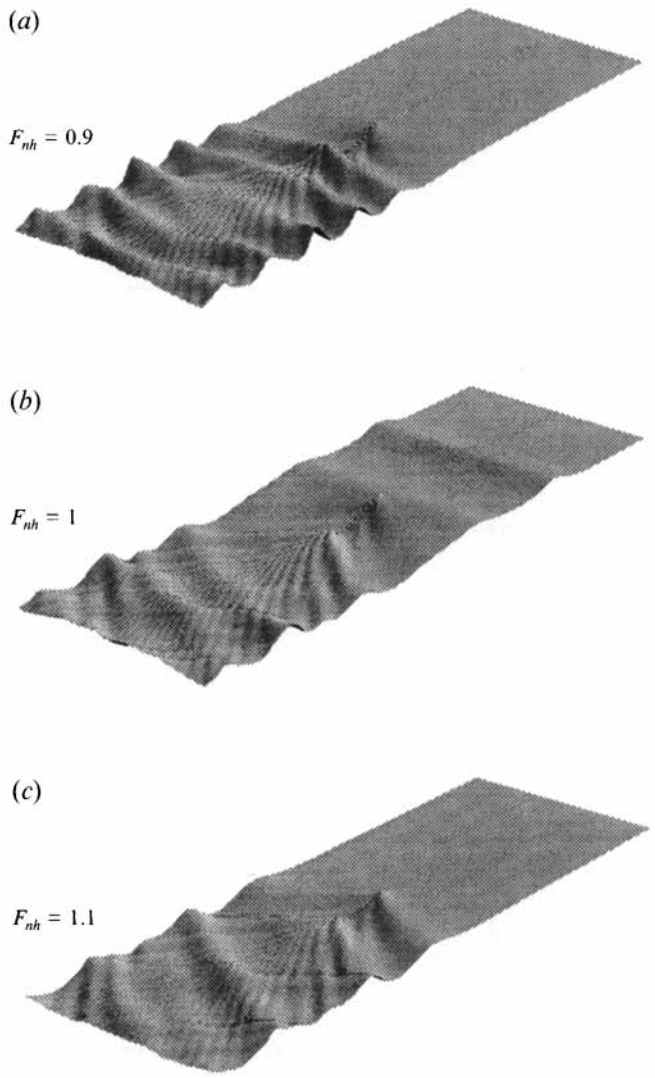

FIGURE 5. Wave patterns at $F_{nh} = 0.9$, $F_{nh} = 1$ and $F_{nh} = 1.1$ for TSS model in case of $h^*/l^* = 0.125$ at $\tau = 10$, where the viewed horizontal area is 30×10.1 m^2 and the vertical scale is exaggerated 10 times.

et al. (1964), but only three water depths $h^*/l^* = 0.208$, 0.167 and 0.125 are examined; the towing mode is free.

We are seeking a useful and reliable computational program for a ship in shallow water. So checking the theoretical predictions of wave resistance, sinkage and trim of the ship by comparison with Graff's results is essential. These quantities are shown as functions of depth Froude number F_{nh} in figures 2–4 for the three water depths, respectively, together with the measured results of Graff *et al.* (1964). Owing to the generation of solitons, the resistance, sinkage and trim vary with time in a certain speed range, so their maximum, minimum and averaged values are indicated in figures 2–4 by vertical bars with dots. The calculations show satisfactory overall agreement with measurements.

Perspective views of the wave pattern for water depth $h^*/l^* = 0.125$ at $F_{nh} = 0.9$,

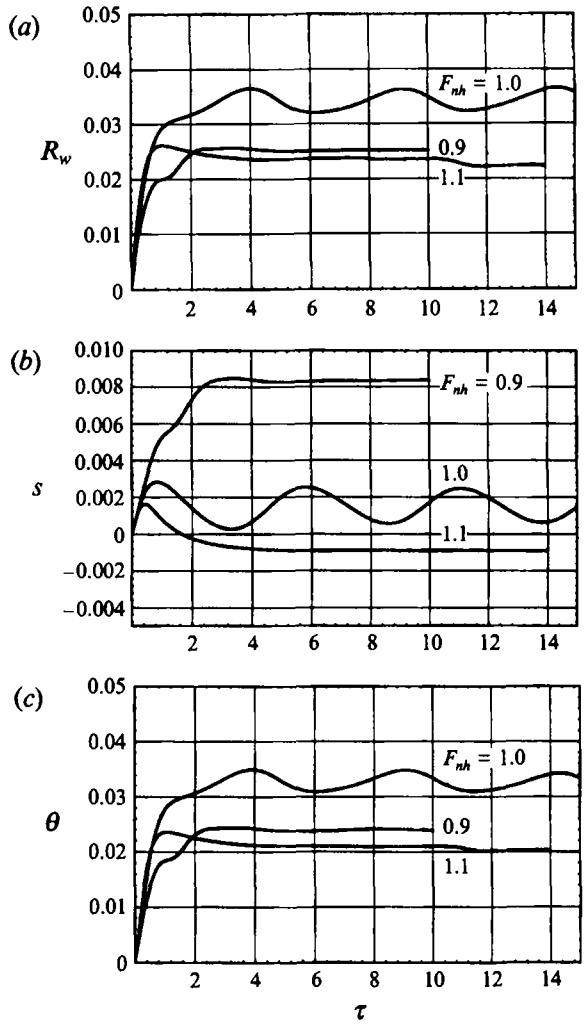

FIGURE 6. Time history of wave resistance, sinkage and trim for TSS model in case of $h^*/l^* = 0.125$ at three depth Froude numbers: 0.9, 1.0 and 1.1.

$F_{nh} = 1$ and $F_{nh} = 1.1$ are shown in figure 5 with the vertical scale exaggerated 10 times for clarity. The patterns in figures 5(*a*) and 5(*c*) have already developed to the steady state, while the pattern in figure 5(*b*) will still vary periodically, further generating solitons. For the same cases the calculated wave resistance, sinkage and trim varying with time are shown in figure 6.

The experiment of Graff *et al.* (1964) is considered as a conventional shallow-water towing tank experiment. The longitudinal blockage parameter, i.e. ratio of midship sectional area to tank water sectional area, is about 10 times smaller in Graff's cases than that in Ertekin's cases. We have seen that the calculated soliton for Graff's case is smaller and flatter, which conforms to the conclusion of previous studies, e.g. Mei (1986), that the amplitude and the wavelength of the upstream solitons depend on the blockage parameter. Moreover, the speed range of soliton generation also depends on this parameter. As we see in figures 2–4, the depth Froude number range of unsteadiness is only about 0.95–1.06 in Graff's cases, that is, much narrower than that reported in Ertekin's experiment.

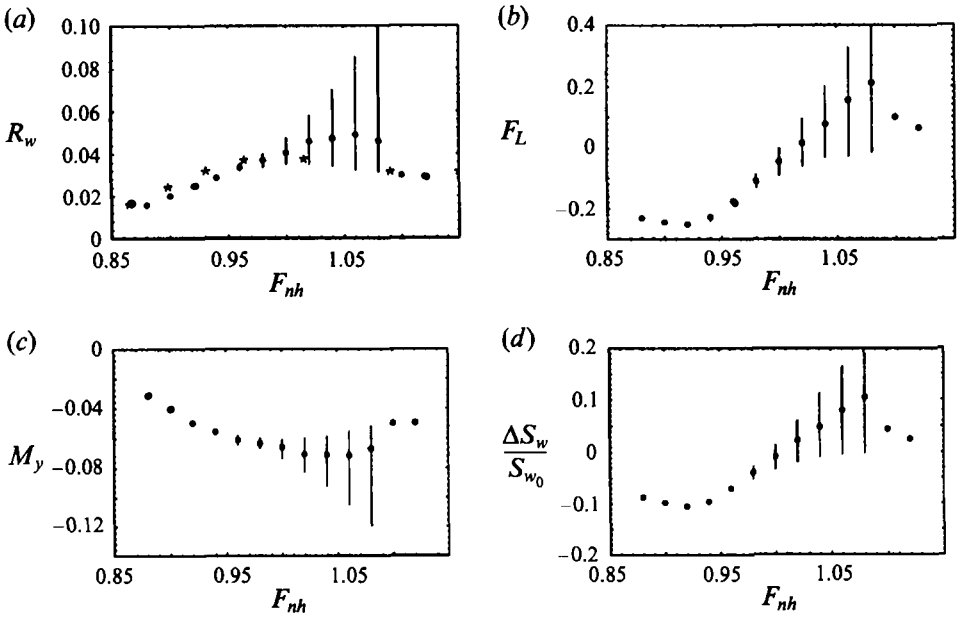

FIGURE 7. Calculated wave resistance, lift force, moment about Oy, and increase of wetted surface area, dots denote the average calculated values, vertical bars represent the range of variation between minimum and maximum in the calculation, and asterisks denote Millward & Bevan's measurements in (*a*) only.

4.3. *Wigley mathematical model*

Being identical to Millward & Bevan's case (1986) the model hull is given by

$$\frac{y^*}{b^*} = \begin{cases} [1-4\hat{x}^2]\left[1-\left(\dfrac{z^*}{d^*}\right)^2\right] & (-d^* \leqslant z^* \leqslant 0) \\ 1-4\hat{x}^2 & (z^* > 0) \end{cases} \qquad (-\tfrac{1}{2} < \hat{x} < \tfrac{1}{2}),$$

where $l^* = 1.905$ m, $b^* = 0.238$ m and $d^* = 0.095$ m. The channel is 6.1 m wide and only one water depth $l^*/h^* = 6$ is selected for calculation. The model is kept fixed in Millward & Bevan (1986) and so is the calculation here.

Our calculated results are shown in figure 7 along with the measured wave resistance of Millward & Bevan. By comparison with their figure 7, it will be found that our calculations are closer to the experiment than theirs in the near-critical speed range, presumably because their prediction is based on linear theory.

5. Concluding remarks

The theoretical model presented in this paper is correct to second order, because it takes the local wave elevation and the longitudinal disturbance velocity into account in the near field. It is not restricted to symmetric configuration of ship and channel. The computational technique used in efficient and of second-order precision. The results obtained agree well with ship model experiments. Several practical applications are being pursued. One is the extension to high-speed twin-hull ships by regarding each hull as moving off-centre in an imaginary channel. Another is hull-form optimization, i.e. determination of lengthwise distribution of cross-sectional area to yield minimum

wave resistance under suitable constraints. Further, the present model can be applied to the practical problem of an air-cushion ship in shallow water, which was also investigated by Ertekin *et al.* (1986) and Katsis & Akylas (1987) with shallow-water wave theory. Finally, it is noted that, although our work here is limited to the near-critical range, the KP equation can be modified for a wider speed range, which is as large as the Boussinesq equations hold for. It can be applied to more practical purposes without any numerical handicap.

X.-N.C. wishes to express his gratitude to the Alexander von Humboldt Foundation for the award of a research fellowship which enabled him to complete this work in Germany at the Mercator University, Duisburg. We thank Dipl.-Ing. B. Kirsten for his valuable help in the use of various computing devices for this work and Dr.-Ing. T. Jiang for his careful scrutiny of all derivations and equations including numerical schemes.

REFERENCES

AKYLAS, T. R. 1984 On the excitation of long nonlinear water waves by a moving pressure distribution. *J. Fluid Mech.* **141**, 455–466.

CHEN, X.-N. 1989 Unified Kadomtsev–Petviashvili equation. *Phys. Fluids* A **1**, 2058–2060.

CHEN, X.-N. & LIU, Y.-Z. 1988 Diffraction of a solitary wave by a thin wedge. *Acta Mechanica Sinica* **4**, 201–210.

CHOI, H.-S., BAI, J.-W., KIM, K. J. & CHO, I.-H. 1990 Nonlinear free surface waves due to a ship moving near the critical speed in a shallow water. *Proc. 18th Symp. Naval Hydrodyn. Ann Arbor*, pp. 173–189.

CHOI, H. S. & MEI, C. C. 1989 Wave resistance and squat of a slender ship moving near the critical speed in restricted water. *Proc. 5th Intl Conf. on Numer. Ship Hydrodyn.*, pp. 439–454.

COLE, S. J. 1985 Transient waves produced by flow past a bump. *Wave Motion* **7**, 579–587.

DAND, I. W. 1973 The squat of full ship in shallow water. *Trans. R. Inst. Nav. Arch.* **115**, 237–255.

ERTEKIN, R. C. 1984 Soliton generation by moving disturbances in shallow water: theory, computation and experiment. PhD thesis, University of California, Berkeley.

ERTEKIN, R. C., WEBSTER, W. C. & WEHAUSEN, J. V. 1985 Ship-generated solitons. *Proc. 15th Symp. Nav. Hydrodyn. Hamburg*, pp. 347–364.

ERTEKIN, R. C., WEBSTER, W. C. & WEHAUSEN, J. V. 1986 Waves caused by a moving disturbance in a shallow channel of finite width. *J. Fluid Mech.* **169**, 275–292.

GERTLER, M. 1954 A reanalysis of the original test data for the Taylor Standard Series. *Report 806, Navy Department, The David W. Taylor Model Basin, Washington 7, DC.*

GRAFF, W. 1962 Untersuchungen über die Ausbildung des Wellenwiderstandes im Bereich der Stauwellengeschwindigkeit in flachem, seitlich beschränktem Fahrwasser. *Schiffstechnik* **9**, 110–122.

GRAFF, W., KRACHT, A. & WEINBLUM, G. 1964 Some extension of D. W. Taylor's standard series. *Trans. Soc. Nav. Arch. Mar. Engrs* **72**, 374–401.

GRIMSHAW, R. H. J. & SMYTH, N. F. 1986 *J. Fluid Mech.* **169**, 429–464.

HUANG, D. B., SIBUL, O. J. & WEHAUSEN, J. V. 1983 Ships in very shallow water. *Festkolloquium zur Emeritierung von Karl Wieghardt, Institut für Schiffbau der Universität Hamburg, Rep.* 427, pp. 29–49.

KATSIS, C. & AKYLAS, T. R. 1987 On the excitation of long nonlinear water waves by a moving pressure distribution. Part 2. Three-dimensional effects. *J. Fluid Mech.* **177**, 49–65.

KINOSHITA, M. 1946 On the restricted-water effect on ship resistance. *Jap. Soc. Nav. Arch.* **150**, 181–187.

KIRSCH, M. 1966 Shallow water and channel effects on wave resistance. *J. Ship Research* **10**, 164–181.

LEA, G. K. & FELDMAN, J. P. 1972 Transcritical flow past slender ships. *Proc. 8th Symp. Nav. Hydrodyn.* Office of Naval Research.

MARUO, H. 1989 Evolution of the theory of slender ships. *Schiffstechnik* **36**, 107–133.

MEI, C. C. 1976 Flow around a thin body moving in shallow water. *J. Fluid Mech.* **77**, 737–751.

MEI, C. C. 1983 *The Applied Dynamics of Ocean Surface Waves.* Wiley-Interscience.

MEI, C. C. 1986 Radiation of solitons by slender bodies advancing in a shallow channel. *J. Fluid Mech.* **162**, 53–67.

MEI, C. C. & CHOI, H. S. 1987 Forces on a slender ship advancing near the critical speed in a wide canal. *J. Fluid Mech.* **179**, 59–76.

MILLWARD, A. & BEVAN, M. G. 1986 Effect of shallow water on a mathematical hull at high subcritical and supercritical speeds. *J. Ship Res.* **30**, 85–93.

NEWMAN, J. N. 1969 Lateral motion of a slender body between two parallel walls. *J. Fluid Mech.* **39**, 97–115.

OGILVIE, T. F. 1976 Wave-length scales in slender-ship theory. *Proc. Intl Seminar on Ship Tech. Hydrodyn. Session in Seoul*, pp. 5.0–22.

SMYTH, N. F. 1986 Modulation theory solution for resonant flow over topography. *Dept of Maths Rep.* 3. University of Melbourne, Victoria, Australia.

TAYLOR, P. J. 1973 The blockage coefficient for flow about an arbitrary body immersed in a channel. *J. Ship Res.* **17**, 97–105.

THEWS, J. G. & LANDWEBER, L. 1935 The influence of shallow water on the resistance of a cruiser model. *US Expl Model Basin, Navy Yard, Washington, DC, Rep.* 408.

THEWS, J. G. & LANDWEBER, L. 1936 A thirty-inch model of the SS Clariton in shallow water. *US Expl Model Basin, Navy Yard, Washington, DC, Rep.* 414.

TODD, F. H. 1953 Some further experiments on single-screw merchant ship forms – Series 60. *Trans. Soc. Nav. Arch. Mar. Engrs* **61**, 519–589.

TOMASSON, G. G. & MELVILLE, W. K. 1991 Flow past a constriction in a channel: a model description. *J. Fluid Mech.* **232**, 21–45.

TUCK, E. O. 1966 Shallow-water flows past slender bodies. *J. Fluid Mech.* **26**, 81–95.

WHITHAM, G. B. 1974 *Linear and Nonlinear Waves.* Wiley.

WU, DE-MING & WU, T. Y. 1982 Three-dimensional nonlinear long waves due to moving surface pressure. *Proc. 14th Symp. Nav. Hydrodyn. Ann Arbor, Mich.*, pp. 103–129.

WU, T. Y. 1987 Generation of upstream advancing solitons by moving disturbances. *J. Fluid Mech.* **184**, 75–99.

YANENKO, N. N. 1971 *The Method of Fractional Steps.* Springer.